

1 Characterising radium-226 particles from legacy contamination to support radiation dose 2 assessments

3
4 C. McGuire ^{a, b, *}, P. Dale ^b, D. Copplestone ^a, C. Wilson ^a and A. Tyler ^a

5
6 ^a Biological and Environmental Sciences, Faculty of Natural Sciences, University of Stirling, Stirling, FK9
7 4LA, United Kingdom

8 ^b Scottish Environment Protection Agency, Strathallan House, Castle Business Park, Stirling, FK9 4TZ,
9 United Kingdom

10
11 * Corresponding author: Corynne McGuire (corynne.mcguire@stir.ac.uk)
12

13 14 Highlights

- 15
- 16 • Particle characterisation data required to support dose assessments is presented
- 17 • Radiological, physical and chemical characterisation of Ra-226 particles is ongoing
- 18 • Characterisation data for one Ra-226 particle is presented as an example
- 19 • Plan to use Ra-226 particle characterisation data in dose assessments is discussed
- 20 • A new radioactive particle definition is needed to support dose assessments
- 21

22 23 Abstract

24
25 Radioactive particles are physically discrete sources of radioactivity that have been released into the
26 environment as a result of past emergencies, events and practices. As the release of radioactive
27 particles is often unplanned, the source term has not been characterised, and the potential radiation
28 doses have not been prospectively assessed. If a plausible exposure pathway exists, radioactive
29 particles in the environment may present a hazard to the public depending on their radiological,
30 physical and chemical characteristics. Given their physically discrete nature, standard assessment
31 approaches such as dispersion and transfer modelling of liquid and gaseous radioactive releases, are
32 not appropriate for radioactive particles. The challenge for national regulatory authorities is to
33 calculate potential radiation doses from unplanned releases of radioactive particles into the
34 environment, assess whether the doses are relevant to radiological protection and decide whether
35 actions are required to reduce potential doses. To address this challenge, this paper presents the
36 approach being adopted to radiologically, physically and chemically characterise Ra-226 particles from
37 a contaminated legacy site using gamma spectrometry, optical macroscopy and SEM-EDS. The use of
38 particle characterisation data to support radiation dose assessments is discussed and consideration is
39 given to radioactive particles in the context of radiological protection.
40

41 42 1. Introduction

43
44 Radioactive particles are physically discrete sources of radioactivity that have been released into the
45 environment as a result of past emergencies, events and practices including nuclear power reactor
46 accidents, accidents involving nuclear weapons, nuclear weapons testing, the use of depleted uranium
47 in military operations and legacy contamination from past practices (IAEA, 2011). As the release of
48 radioactive particles is often unplanned, the source term has not been characterised and the potential
49 radiation doses have not been prospectively assessed. If a plausible exposure pathway exists,
50 radioactive particles in the environment may present a hazard to the public depending on their
51 radiological, physical and chemical characteristics. Given their physically discrete nature, standard

52 assessment approaches such as dispersion and transfer modelling of liquid and gaseous radioactive
53 releases, are not appropriate for radioactive particles (Dale et al., 2008). The challenge for national
54 regulatory authorities is to calculate potential radiation doses from unplanned releases of radioactive
55 particles into the environment, assess whether the doses are relevant to radiological protection and
56 decide whether actions are required to reduce potential doses.

57 58 *1.1. Radioactive particles in radiological protection* 59

60 The International System of Radiological Protection, as published and maintained by the International
61 Commission on Radiological Protection (ICRP), considers three different types of radiation exposure
62 situation intended to encompass all possible circumstances where radiation exposure could occur:
63 planned, emergency and existing. Existing exposure situations, relevant to unplanned releases of
64 radioactive particles, are exposure situations that already exist when a decision on control must be
65 taken. That decision could be to take action to reduce potential radiation doses, such as
66 implementation of remediation strategies or site management controls, or to do nothing if such action
67 is not warranted (ICRP, 2007). This should be done in accordance with a graded approach to ensure
68 any decisions or actions taken are commensurate with the radiation risks associated with the exposure
69 situation (IAEA, 2014).

70
71 Existing exposure situations include exposures that exist due to past emergencies, events or practices
72 as well as naturally occurring exposures. The level of radiological protection in existing exposures
73 situations is defined by the reference level, which is the level of dose or risk, above which it is judged
74 to be inappropriate to plan to allow exposures to occur, and below which optimisation of protection
75 should be implemented. The reference level is not prescribed by the ICRP but should be set by
76 national regulatory authorities taking into account the prevailing circumstances of the existing
77 exposure situation under consideration (ICRP, 2007).

78
79 Unlike planned exposure situations where the radiation source term is already characterised, and the
80 potential radiation doses prospectively assessed against dose limits and constraints, the source term
81 in an existing exposure situation is often not well characterised due to its unplanned nature (Dale et
82 al., 2008). In these circumstances, data on the source term characteristics, including any radioactive
83 particles present, need to be obtained to undertake an assessment of potential radiation doses against
84 the reference level and take appropriate actions, if necessary.

85
86 A significant amount of research has been undertaken to characterise radioactive particles from a
87 number of existing exposure situations that have arisen due to past emergencies, events and
88 practices: nuclear power reactor accidents at Chernobyl, Ukraine (Pöml and Burakov, 2017; Shiryayev
89 et al., 2018) and Fukushima, Japan (Kaltofen and Gundersen, 2017; Martin et al., 2016; Yamaguchi et
90 al., 2016); accidents involving nuclear weapons at Palomares, Spain (Aragón et al., 2008; Jimenez-
91 Ramos et al., 2010; Jiménez-Ramos et al., 2012, 2008, 2006; Lind et al., 2007; López et al., 2007;
92 Pöllänen et al., 2006) and Thule, Greenland (Eriksson et al., 2005; Lind et al., 2005); nuclear weapons
93 testing (Burns et al., 1995; Conway et al., 2009; Jernström et al., 2006); the use of depleted uranium
94 in military operations (Lind et al., 2009; Sajih et al., 2010; Salbu et al., 2005, 2003; Török et al., 2004);
95 and legacy contamination from past practices at Sellafield, England (Clacher, 2011, 2010; Cowper,
96 2009), Dounreay (Aydarous et al., 2008; J. Darley et al., 2003) and Dalgety Bay, Scotland (Wilson et al.,
97 2013).

98
99 The next step is to use the data from radioactive particle characterisation studies to calculate potential
100 radiation doses, which will allow the assessment of the existing exposure situations against the
101 reference level and, if necessary, implementation of remediation strategies or site management
102 controls to reduce potential radiation doses in accordance with a graded approach.

103

104 *1.2. Existing exposure situation at Dalgety Bay, Scotland*

105

106 A significant amount of work has been undertaken by, and on behalf of, the Scottish Environment
107 Protection Agency (SEPA) to address the existing exposure situation at Dalgety Bay, which is an
108 estuarine bay located on the north bank of the Firth of Forth estuary in Scotland (Figure 1).
109 Radioactive particles, containing Ra-226 and associated alpha-, beta- and gamma-emitting daughter
110 radionuclides, were first discovered on the beach at Dalgety Bay in 1990 and originate from past
111 practices undertaken on the land adjacent to the bay by the UK Ministry of Defence (MoD). The land
112 was host to MoD air force activities (RNAS Donibristle and HMS Merlin) between 1917 and 1959, a
113 time when Ra-226 was used in paint to luminise aircraft components (Patton, 2013). Activities on the
114 land left a legacy of radioactive contamination and SEPA has been undertaking regular radiological
115 monitoring surveys that have collectively recovered >1000 radioactive particles, varying greatly in
116 physical size and Ra-226 activity (approx. 1kBq - 76MBq).

117

118 The existing exposure situation at Dalgety Bay was assessed by SEPA in 2013 (Dale, 2013). The
119 assessment concluded there is a significant possibility of members of the public receiving radiation
120 doses via skin contact and inadvertent ingestion above the relevant reference levels as defined in The
121 Radioactive Contaminated Land (Scotland) Regulations 2007 Statutory Guidance (Scottish
122 Government, 2010). As a result, the MoD is implementing a remediation strategy, meanwhile site
123 management controls, such as signage and site demarcation, are being maintained by SEPA to protect
124 the public.

125

126 As part of this assessment, SEPA commissioned a number of ad hoc research studies to provide the
127 underpinning data for the skin contact and inadvertent ingestion dose calculations, as well as
128 highlighting limitations and knowledge gaps requiring further research. Skin dose modelling was
129 undertaken to estimate potential skin doses but, due to the lack of particle characterisation data, a
130 point source geometry was assumed. This approach neglected the impact of self-absorption of
131 radiation within the particles leading to an overestimation of skin dose, particularly for the alpha and
132 beta emissions (Charles, 2008). Consequently, direct measurements of potential skin doses were
133 undertaken using radiochromic film (RCF) dosimetry for ten particles. Improved skin dose modelling
134 would have required details of the size, shape, density, chemical composition and radionuclide
135 content, which were not available (Charles and Gow, 2010). The direct measurements demonstrated
136 the impact of self-absorption, as the measured doses were significantly lower than the previously
137 modelled doses. The beta emissions were the dominant contributor to skin dose, with a potential
138 contribution from the alpha emissions at shallow skin depths, although the RCF was not specifically
139 calibrated for alpha emissions (Charles and Gow, 2010). Additionally, the particle activity
140 measurements reported in both studies are subject to significant uncertainty (15 - 30%), contributing
141 to the overall uncertainty of the skin dose estimates.

142

143 Simulated gastrointestinal digestion was undertaken using sixty particles for calculating doses from
144 inadvertent ingestion and found a wide range of gastrointestinal solubility (1 – 35% of particle activity)
145 but, due to the lack of particle characterisation data, the cause of such a wide range could not be
146 investigated. The percentage solubilities reported are also subject to significant uncertainty due to
147 the 25% uncertainty on the particle activity measurements (Tyler et al., 2013).

148

149 A sample of nine particles was radiologically, physically and chemically characterised with the aim of
150 investigating their origin, deposition and transport within the local environment at Dalgety Bay
151 (Wilson et al., 2013). The analyses reported a range of activities, sizes, shapes and chemical
152 composition, and alluded to the presence of distinct sub-populations, but the limited sample size did
153 not allow for statistically robust conclusions. Additionally, these particles were different to those used

154 in the skin and ingestion dose studies (Charles, 2008; Charles and Gow, 2010; Tyler et al., 2013),
155 therefore the influence of particle characteristics on skin and ingestion doses could not be
156 investigated.

157
158 An improved understanding of the hazard presented by the Ra-226 particles is not only important for
159 the work ongoing at Dalgety Bay but also other sites potentially contaminated due to past practices
160 using radium as well as existing exposure situations involving radioactive particles from other sources.
161 It is important to understand the particle characteristics that influence radiation doses and to have a
162 suitable level of confidence in radiation dose assessments for ensuring that existing exposure
163 situations are assessed appropriately, and for implementing appropriate remediation strategies or site
164 management controls.

165

166 *1.3. Research Aim & Objectives*

167

168 The aim of this paper is to highlight the research currently underway to radiologically, physically and
169 chemically characterise a representative sample of Ra-226 particles from Dalgety Bay, creating particle
170 profiles containing the necessary data to support radiation dose assessments. Research objectives
171 address the limitations and knowledge gaps identified in previous research, specifically to:

172

- 173 i. Radiologically, physically and chemically characterise a larger sample of Ra-226 particles;
- 174 ii. Improve particle activity estimates by reducing the uncertainty in activity measurements;
- 175 iii. Assess potential skin contact doses through improved measurement and modelling, and
176 investigate the particle characteristics having the greatest influence on skin doses;
- 177 iv. Assess potential inadvertent ingestion doses and investigate the particle characteristics
178 influencing gastrointestinal solubility; and
- 179 v. Determine whether there are any distinct sub-populations of particles that have common
180 characteristics, consider their provenance and distribution in the environment and any
181 implications for the development of remedial measures and the management controls
182 currently in place.

183

184 The research introduced in this paper addresses research objectives (i) and (ii) and methods are
185 currently under development to address research objectives (iii), (iv) and (v).

186

187 More broadly, this paper builds on the significant amount of research already published on radioactive
188 particle characterisation and discusses the next step of using the data generated from characterisation
189 studies to calculate potential radiation doses. Taking this next step allows for the assessment of
190 existing exposure situations against the reference level and, if necessary, implementation of
191 remediation strategies or site management controls to reduce potential radiation doses in accordance
192 with a graded approach.

193

194

195 **2. Materials and Methods**

196

197 Radiological, physical and chemical characterisation of a representative sample of Ra-226 particles is
198 underway using a variety of analytical techniques. The particles have been selected from those
199 recovered during the monitoring surveys undertaken by SEPA based on in-field estimates of Ra-226
200 activity and physical size. Each particle is undergoing the same suite of analyses to produce particle
201 profiles containing the necessary data to support radiation dose assessments.

202

203 *2.1. Radiological Characterisation*

204

205 The radioactivity content of each particle is analysed by gamma spectrometry. The analysis is using
206 an Ortec Gamma-X (GMX) N-Type High Purity Germanium (HPGe) Coaxial Photon Detector linked to
207 Ortec Gamma Vision Software for spectrum analysis. Due to the irregular geometries of the Ra-226
208 particles, efficiency calibrations associated with standard sample geometries, such as Marinelli
209 beakers, are not appropriate. To minimise the impact of the irregular geometries, an efficiency
210 calibration has been derived that is as independent from sample geometry as possible (Tyler et al.,
211 2013). Using two gamma reference point sources, Ra-226 (100kBq, UR371, Eckert & Ziegler) and Pb-
212 210 (231kBq, KU654, AEA Technology), a particle-specific efficiency calibration has been derived at
213 distance from the detector (20cm), allowing the Ra-226 particles to behave as point sources,
214 minimising the effect of sample geometry. The particle-specific efficiency calibration has been quality
215 checked using a different gamma reference point source, Eu-152 (43.8kBq, AF4331, Eckert & Ziegler).

216
217 Using the particle-specific efficiency calibration, each particle is counted at 20cm above the detector
218 until the counting uncertainty (2σ) is <5% to determine the activity of Ra-226 and its gamma-emitting
219 daughter radionuclides Pb-214, Bi-214 and Pb-210. The particles are counted in plastic pots, which
220 are closed with a lid but not hermetically sealed.

221 222 *2.2. Physical Characterisation*

223
224 The size and shape of each particle is analysed by optical macroscopy. The analysis is using a Leica
225 M420 optical microscope fitted with an Olympus ColourView III digital camera linked to the Olympus
226 Stream Image Analysis Software for image acquisition, processing and measurement. The microscope
227 is calibrated for a range of magnifications (5.8x, 8x, 10x, 12.5x, 16x, 20x, 25x and 35x) in order to
228 analyse a range of particle sizes. Each magnification is calibrated using a stage micrometer and a
229 quality check is performed before and after each batch of particles is analysed using a reference
230 object. The dimensions of the reference object have been accurately measured using a set of
231 calibrated Vernier callipers.

232
233 Each particle is placed on the microscope stage beneath the objective lens under oblique incident
234 illumination from two opposing directions to minimise shadows. The most appropriate magnification
235 is selected, and adjustments made to the white balance and exposure. Due to the irregular geometry
236 of the particles, images are acquired using the manual Extended Focal Imaging (EFI) function in Stream,
237 which acquires multiple images at different focal points and combines them into a single image with
238 the whole particle in focus. Once the EFI is captured, the image is segmented using HSV thresholding
239 to separate the particle from the image background, allowing the software to make the required size
240 and shape measurements. Each particle is imaged in multiple orientations, at least three if possible,
241 in order to calculate average size and shape parameters for each particle. However, due to the nature
242 of their production and time spent in the environment, the shape of the particles varies considerably.
243 Depending on their shape, some particles are more amenable to imaging in different orientations than
244 others, and may have images taken in greater, or fewer, than three orientations. A total of 10 different
245 size (radius, diameter, equivalent circular diameter, area and perimeter) and shape (shape factor,
246 sphericity, aspect ratio, elongation, convexity) measurements are taken for each orientation. The
247 individual measurements for each orientation are recorded as well as the mean and standard
248 deviation of all orientations of the particle. Qualitative observations are also made such as the
249 presence of void spaces and particle friability.

250
251 The mass of each particle is measured using an Oxford GM-2505D 5-figure laboratory balance. The
252 balance is calibrated annually by a UKAS accredited calibration service and the calibration is checked
253 before and after each batch of particles is measured. The check is performed using a set of calibration
254 weights (1, 10 and 100mg; Kern & Sohn) manufactured to International Organisation of Legal
255 Metrology (OIML) standards. Each calibration weight is measured in triplicate to ensure the balance

256 is performing correctly. The mass of each particle is measured once, and the result recorded when
257 the balance has stabilised.

258

259 *2.3. Chemical Characterisation*

260

261 The surface chemical composition of each particle is analysed by scanning electron microscopy with
262 energy dispersive X-ray spectroscopy (SEM-EDS). The analysis is using a Zeiss EVO MA-15 variable
263 pressure SEM fitted with a backscattered electron (BSE) detector, a secondary electron (SE) detector,
264 a variable pressure secondary electron (VPSE) detector and an Oxford Instruments X-Max 80mm² SDD
265 EDS detector. The BSE detector is positioned directly above the microscope stage whereas the SE,
266 VPSE and EDS detectors are positioned at an angle (approx. 30°) relative to the stage. The SEM is using
267 Zeiss SmartSEM Software for BSE, SE and VPSE image acquisition and Oxford Instruments AZtec
268 Software for EDS analysis. The SEM-EDS is calibrated annually by the manufacturer using a multi-
269 element standard and a quality check is performed before and after each batch of particles is analysed
270 using a cobalt standard.

271

272 The particles are mounted on standard 12.5mm diameter aluminium SEM pin stubs using carbon
273 adhesive disks. The particles are not subject to any sample preparation, such as the application of a
274 conductive coating or polishing, in order to preserve their original characteristics for the subsequent
275 analyses required for the assessment of potential radiation doses. As the particles are uncoated, the
276 analysis was performed under low vacuum conditions to help prevent the accumulation of
277 electrostatic charge on the particle surface (Wilson et al., 2013).

278

279 Each particle is imaged in a single orientation using the BSE detector to gather qualitative information
280 on surface chemical composition based on atomic number (*Z*), where areas composed of high-*Z*
281 elements appear brighter than areas composed of low-*Z* elements. SE and VPSE images are acquired
282 to gather qualitative information on surface topography, revealing surface features and areas of the
283 particle surface that are in shadow relative to the SE, VPSE and EDS detector positions. The EDS is
284 used to gather information on surface chemical composition, identifying individual elements to
285 produce element distribution maps and calculating element abundance (weight %). Carbon is
286 excluded from the EDS analysis due to interference from the carbon adhesive disks.

287

288 Due to the irregular geometry of the particles creating shadows, and to allow inter-particle
289 comparison, the surface chemical composition data is collected semi-quantitatively to show the
290 relative abundance of elements on the surface of the particles. Three different types of spectra are
291 acquired for each particle: a particle spectrum acquired from the entire surface of the particle facing
292 the detector; phase spectra acquired from areas on the particle surface where elements appear to be
293 heterogeneously distributed, forming a distinct phase; and point spectra acquired from areas on the
294 particle surface where elements appear to be highly localised. Each spectrum provides element
295 abundance data (weight %) for the part of the particle surface from which the spectrum is acquired.

296

297

298 **3. Results**

299

300 Whilst the analysis is underway for the full representative sample of Ra-226 particles, the complete
301 particle profile for one sample, DBP-03-07, is presented as an example.

302

303 *3.1. Radiological Characterisation*

304

305 The results of the gamma spectrometry analysis for DBP-03-07 show the presence of Ra-226 (5.97kBq
306 ± 6.77%) and its gamma-emitting daughter radionuclides Pb-214 (5.65kBq ± 6.04%), Bi-214 (5.57kBq

307 ± 6.06%) and Pb-210 (4.77kBq ± 8.39%). The particle-specific calibration has significantly reduced the
308 total uncertainties (2σ) to <7%, compared to previous studies (Charles, 2008; Charles and Gow, 2010;
309 Tyler et al., 2013). Pb-210 is the only exception due to the higher activity uncertainty of the Pb-210
310 source used in the efficiency calibration. The radionuclide with the greatest activity is Ra-226, closely
311 followed by Pb-214 and Bi-214, with the lowest activity attributable to Pb-210. Considering the total
312 uncertainties, the activities of Ra-226, Pb-214 and Bi-214 could be in secular equilibrium, whereas the
313 Pb-210 is not due to its activity being significantly lower than the other radionuclides.

314

315 *3.2. Physical Characterisation*

316

317 The results of the optical macroscopy analysis for DBP-03-07 are presented in Figure 2, showing the
318 images generated from the EFI, and in Tables 1 and 2, showing the size and shape measurements
319 obtained from the image analysis. DBP-03-07 had EFI's taken in five different orientations at 25x
320 magnification. The images reveal the irregular shape of the particle, which is different in all five
321 particle orientations. All images show the presence of void spaces within the particle and there is
322 evidence of its deposition in a coastal environment with what appears to be sand grains embedded in
323 some of the voids in images 1 and 5. The particle did not show a tendency to be friable and appeared
324 to be physically robust, although this was under the careful handling of laboratory conditions.

325

326 The size measurements indicate that the particle has a mean diameter of 2.5mm. The size
327 measurement showing the greatest variation is the perimeter, reflecting the irregular geometry,
328 which is supported by the low shape factor. The sphericity and convexity factors are <1 indicating the
329 extent to which the particle deviates from a perfect sphere, which is supported by the aspect ratio
330 and elongation factor both being >1. The particle mass was measured as 0.01232g.

331

332 *3.3. Chemical Characterisation*

333

334 The results of the SEM-EDS analysis for DBP-03-07 are presented in Figure 3, showing the BSE, SE and
335 VPSE images, Figure 4, showing the EDS element maps and Table 3, showing the relative abundance
336 of each element in the particle (weight %). The BSE image reveals distinct high-Z and low-Z regions
337 across the particle surface and the SE and VPSE images reveal a rough surface topography. The EDS
338 element maps reveal the presence of several different elements, some of which appear to be
339 homogenous (excluding shadows), whereas others appear to be heterogeneous by either forming
340 distinct phases or being highly localised. The particle orientation in the SEM-EDS analysis appears to
341 be most closely aligned with the orientation in image 2 from the optical macroscopy, but notably not
342 the same.

343

344 Oxygen (O) appears to be homogeneous, which is confirmed in the relative abundance data where it
345 is consistently high across all spectra and is always the most abundant. Silicon (Si) also appears to be
346 homogeneous across all spectra except for a few significantly brighter, highly localised areas in the Si
347 map. These were investigated using point spectra and, based on their chemical composition, are likely
348 to be embedded sand grains, although this is not as obvious in image 2 of Figure 2 compared to images
349 1 and 5. Iron (Fe) is another element that appears to be present across the particle as it is present in
350 all spectra but it is also forming a distinct phase as can be seen from the Fe map and the high relative
351 abundance of 26.9% in the Fe phase spectrum compared to all other spectra. The map for aluminium
352 (Al) also appears to be homogeneous and this is reflected in the relative abundance data with the
353 exception of the absence of Al in the copper (Cu) and chlorine (Cl) phases.

354

355 All other significant elements appear to be heterogeneous by either forming distinct phases or being
356 highly localised. The Cu and Cl maps are interesting as these elements appear to be at least partly co-
357 located, likely as copper (II) chloride, which is supported by the optical macroscopy image where a

358 blue/green colouration can be seen. However, the Cu is more widely distributed than the Cl. Calcium
359 (Ca) is another element that appears to be present throughout the particle but also forming a distinct
360 phase, as supported by the element abundance data. The tin (Sn) map is particularly interesting as
361 the Sn is present in a distinct phase that can be easily identified as the high-Z area in the BSE image.
362 The Sn is very localised, only appearing in one other spectrum (excluding the particle spectrum).
363 Titanium (Ti) is even more highly localised appearing as a distinct point on the element distribution
364 map.

365
366

367 **4. Discussion**

368

369 Although the results presented are for one particle as an example, there are some initial observations
370 with potential implications for the planned future work to support radiation dose assessments. The
371 significance of the following observations will be clearer when the full set of particle characterisation
372 data is available and will be considered in the subsequent dose assessment work, as appropriate.

373

374 *4.1. Radiological Characterisation*

375

376 In the gamma spectrometry results, it was noted that the activity of Pb-210 is significantly lower than
377 the other radionuclides; there are a number of reasons why this might be the case. Firstly, due to the
378 physical half-life of Pb-210 (22.3 years) and the potential age of the Ra-226 present in the particles,
379 the Pb-210 will have not yet reached secular equilibrium. For example, if it were assumed that the
380 Ra-226 was pure when used to make the paint and the particles are 70 years old, the Pb-210 would
381 have only reached approximately 90% of its secular equilibrium activity at the time of analysis.

382

383 Secondly, the 46.54keV Pb-210 photon is the lowest energy of all photons included in the analysis
384 meaning it is the most susceptible to self-absorption within the particle and may never reach the
385 detector. This is due to the photoelectric effect, which is highly dependent on the effective atomic
386 number of the absorbing material. The impact of this is mitigated to some extent by the Pb-210
387 reference source used in the efficiency calibration where the Pb-210 is sealed in a Perspex disk and
388 due to the particle having a small physical size. However, differences in chemical composition and
389 density of the Pb-210 source and the particle will result in different photoelectric cross-sections for
390 the 46.54keV photons.

391

392 Lastly, the daughter radionuclide immediately after Ra-226 in the decay chain is Rn-222, which is
393 gaseous. If some Rn-222 is able to escape from the particle this would result in all subsequent
394 daughter radionuclides, including Pb-210, having a lower activity and never reaching secular
395 equilibrium with Ra-226. The activities of Pb-214 and Bi-214 are both slightly lower than Ra-226, which
396 could suggest a slight disequilibrium due to a small amount of Rn-222 loss. However, considering the
397 total uncertainties, the activities of Pb-214 and Bi-214 could be in secular equilibrium with Ra-226.
398 Either way, the fact that the measured activities of Pb-214 and Bi-214 are high indicates that even if
399 there is some loss of Rn-222 it will be a small amount and is unlikely to be a significant contributor to
400 the lower Pb-210 activity.

401

402 In addition to Rn-222, it is important to note that there will be other Ra-226 daughter radionuclides
403 present in the particles not identified in the gamma spectrum; Po-218, Po-214, Bi-210 and Po-210.
404 Due to the short physical half-lives of Po-218 and Po-214, they will also be in secular equilibrium with
405 Ra-226 (or Rn-222 if some is being lost). However, as Bi-210 and Po-210 are after Pb-210 in the decay
406 chain, these radionuclides will be in secular equilibrium with the Pb-210 rather than the Ra-226. It is
407 important to consider this in a dose assessment of the Ra-226 particles, which must take account of
408 the full decay chain, as all the radionuclides will contribute to the dose to a greater or lesser extent.

409

410 4.2. *Physical Characterisation*

411

412 In the optical macroscopy results, the irregular shape and the presence of void spaces in the particle
413 was noted. Although the particle did not show a tendency to be friable under laboratory conditions,
414 due to its irregular shape and multiple void spaces, it could be friable if it were left to persist in the
415 environment where it would be subject to physical and chemical weathering processes. Particle
416 friability is a potentially significant consideration when deciding whether to undertake remedial
417 actions and the subsequent development of remediation strategies. Friable particles may not present
418 a plausible exposure pathway in their current form due to their physical size but may do so in future
419 if left to persist in the environment. Weathering processes can break down particles into smaller
420 fragments, potentially altering the exposure pathways by creating particles that may more easily
421 adhere to the skin, may be more easily inadvertently ingested or, if sufficiently small, inhalable.
422 Additionally, the presence of void spaces could have an impact on inadvertent ingestion doses by
423 providing an increased surface area for interaction with gastrointestinal fluids.

424

425 4.3. *Chemical Characterisation*

426

427 An important observation from the SEM-EDS results is that the EDS did not detect Ra-226 or any of its
428 daughter radionuclides in DBP-03-07. This was also reported in Wilson et.al (2013) for all particles
429 included in the analysis and was attributed to the detection limit of the EDS being too high, which is
430 also likely to be the case here. However, despite not detecting it, the heterogeneous distribution of
431 some of the other elements on the particle surface could be an indication that the Ra-226, and
432 associated daughter radionuclides, are also heterogeneously distributed. Intra-particle activity
433 heterogeneity could have important implications for radiation dose assessments as skin contact doses
434 could be more localised than suggested by particle size. Furthermore, this could be important for
435 friable particles where the particle activity would not be equally distributed between the separate
436 fragments after particle breakdown. In terms of inadvertent ingestion dose, the activity could be
437 more, or less, available for gastrointestinal absorption depending on whether the activity is localised
438 on the surface or distributed throughout the particle. Skin contact doses will also be affected by this
439 whereby self-absorption of the emissions would be greater for activity distributed throughout the
440 particle compared to activity localised on the particle surface.

441

442 4.4. *Future work to support radiation dose assessments*

443

444 Once the planned programme of Ra-226 particle characterisation is complete, the radiological,
445 physical and chemical characterisation data will be used in the assessment of potential radiation doses
446 to the public via skin contact and inadvertent ingestion; the most significant exposure pathways at
447 Dalgety Bay.

448

449 To address research objective (iii), a skin contact dose model for the Ra-226 particles is being
450 developed using the Monte Carlo N-Particle (MCNP) radiation transport code. The mass, size, and
451 shape data from the physical characterisation as well as the elemental composition data from the
452 chemical characterisation are being used to parameterise the model. Direct measurements of skin
453 contact doses will be undertaken using radiochromic film (RCF) dosimetry. Once validated by the
454 direct measurements, the skin dose model will be used to explore the influence of different particle
455 characteristics on skin doses. The reduced uncertainty on the particle activity measurements will
456 reduce the overall uncertainty of the skin contact dose calculations providing greater confidence in
457 skin dose assessments.

458

459 To address research objective (iv), the particles are being analysed by simulated gastrointestinal
460 digestion to determine the gastrointestinal solubility of the particles, allowing for the calculation of
461 potential inadvertent ingestion doses. The mass, size, and shape data from the physical
462 characterisation as well as the elemental composition data from the chemical characterisation will be
463 used to explore the influence of different particle characteristics on gastrointestinal solubility. The
464 reduced uncertainty on the particle activity measurements will reduce the overall uncertainty of the
465 gastrointestinal solubility measurements providing greater confidence in inadvertent ingestion dose
466 assessments.

467

468 To address research objective (v), the full suite of particle characterisation data will be used to
469 investigate whether there are any distinct sub-populations with common characteristics, as alluded to
470 by Wilson et al. (2013), consider their provenance and distribution in the environment and any
471 implications for the implementation of remediation strategies or site management controls. An
472 improved understanding of the hazard presented by the Ra-226 particles is not only important for the
473 work ongoing at Dalgety Bay but also other sites potentially contaminated due to past practices using
474 radium as well as existing exposure situations involving radioactive particles from other sources.

475

476 The particle characterisation data and its planned use in radiation dose assessment introduced here
477 for the Ra-226 particles could serve as an example of how it could be applied to particles in other
478 existing exposures situations. To facilitate this, a definition of radioactive particles in the context of
479 radiological protection and in accordance with a graded approach is needed. The International Atomic
480 Energy Agency (IAEA) currently defines radioactive particles as “...a localized aggregation of
481 radioactive atoms that give rise to an inhomogeneous distribution of radionuclides significantly
482 different from that of the matrix background.” (IAEA, 2011). However, this is neither in the context of
483 radiological protection nor in accordance with a graded approach.

484

485 As detailed earlier, the level of radiological protection in existing exposures situations is defined by
486 the reference level, which is the level of dose or risk above which it is judged to be inappropriate to
487 plan to allow exposures to occur, and below which optimisation of protection should be implemented.
488 Consequently, for a definition of radioactive particles to be in the context of radiological protection,
489 it must focus on the hazard presented by radioactive particles and the potential radiation doses, rather
490 than their inhomogeneity relative to the matrix background. As the current IAEA definition is focused
491 on the matrix background, it is not in the context of radiological protection and is driving the
492 consideration of all radioactive particles, regardless of their hazard, which is not in accordance with a
493 graded approach.

494

495 A new definition of radioactive particles is needed to ensure that the management of existing
496 exposure situations involving radioactive particles is relevant to radiological protection and in
497 accordance with a graded approach. Such a definition could be set in relation to the reference level
498 as this would address the needs of national regulatory authorities and allow for the proper
499 implementation of the international system of radiological protection. If individual radioactive
500 particles could deliver doses above the reference level, these particles would require a particle-specific
501 dose assessment to be undertaken. If individual particles could not deliver doses above the reference
502 level, these particles could be considered as particulate contamination, of which consideration is only
503 needed regarding the rate of release of the radioactivity from the particles. These particles do not
504 require a particle-specific dose assessment as, once radioactivity is released from the particles,
505 standard distribution coefficients and/or concentration ratios would apply. Such a definition would
506 ensure that the management of existing exposure situations involving radioactive particles is relevant
507 to radiological protection and in accordance with a graded approach.

508

509

510 **5. Conclusions**

511

512 The particle profile for one Ra-226 particle from Dalgety Bay has been presented and discussed to
513 highlight the radiological, physical and chemical characterisation underway and how these data will
514 be used in radiation dose assessments. Once the particle profiles are complete for the full sample of
515 Ra-226 particles, the characterisation data will be used to improve radiation dose calculations and
516 understand the particle characteristics that influence skin contact and inadvertent ingestion doses.
517 An improved understanding of the hazard presented by the Ra-226 particles is not only important for
518 the work ongoing at Dalgety Bay but also other sites potentially contaminated due to past practices
519 using radium as well as existing exposure situations involving radioactive particles from other sources.

520

521 More broadly, there is a significant body of work already published characterising radioactive particles
522 from a variety of sources and the next step is to use the data from radioactive particle characterisation
523 studies to calculate potential radiation doses. This will allow for the assessment of existing exposure
524 situations against the reference level and, if necessary, implementation of remediation strategies or
525 site management controls to reduce potential radiation doses in accordance with a graded approach.
526 The programme of research discussed in this paper on the Ra-226 particles from Dalgety Bay provides
527 an example of how to take this next step and the same approach could be applied to other existing
528 exposure situations. However, a new definition of radioactive particles is needed to ensure that the
529 management of existing exposure situations involving radioactive particles is relevant to radiological
530 protection and in accordance with a graded approach.

531

532

533 **Declaration of competing interests**

534

535 The authors declare that they have no known competing financial interests or personal relationships
536 that could have appeared to influence the work reported in this paper.

537

538

539 **Acknowledgements**

540

541 I gratefully acknowledge the help I received from Stuart Bradley (University of Stirling) in using the
542 gamma spectrometers, George McLeod (University of Stirling) in using the SEM-EDS and Dr Paul
543 Adderley (University of Stirling) in using the optical microscope. I would like to thank the Scottish
544 Environment Protection Agency and the University of Stirling for funding this research.

545

546

547 **References**

548

549 Aragón, A., Espinosa, A., de la Cruz, B., Fernández, J.A., 2008. Characterization of radioactive
550 particles from the Palomares accident. *J. Environ. Radioact.* 99, 1061–7.

551 <https://doi.org/10.1016/j.jenvrad.2007.12.014>

552 Aydarous, A.S., Charles, M.W., Darley, P.J., 2008. Dose distribution measurements and calculations
553 for Dounreay hot particles. *Radiat. Prot. Dosimetry* 128, 146–158.

554 <https://doi.org/10.1093/rpd/ncm328>

555 Burns, P.A., Cooper, M.B., Lokan, K.H., Wilks, M.J., Williams, G.A., 1995. Characteristics of plutonium
556 and americium contamination at the former U.K. atomic weapons test ranges at Maralinga and

557 Emu. *Appl. Radiat. Isot.* 46, 1099–1107. [https://doi.org/10.1016/0969-8043\(95\)00153-5](https://doi.org/10.1016/0969-8043(95)00153-5)

558 Charles, M.W., 2008. Skin dose from Ra-226 contamination : Dose estimation & comments,
559 University of Birmingham.

560 Charles, M.W., Gow, C., 2010. Skin dose from Dalgety Bay Ra-226 contamination : Dose rate

561 measurements for ten selected samples, University of Birmingham.
562 Clacher, A., 2011. Analysis of Beach Monitoring Finds – Third Tranche: Report to Sellafield Limited,
563 Serco.
564 Clacher, A., 2010. Analysis of Beach Monitoring Finds - Second Tranche: Report to Sellafield Limited,
565 Serco.
566 Conway, M., León Vintro, L., Mitchell, P.I., García-Tenorio, R., Jimenez-Ramos, M.C., Burkitbayev, M.,
567 Priest, N.D., 2009. In-vitro analysis of the dissolution kinetics and systemic availability of
568 plutonium ingested in the form of “hot” particles from the Semipalatinsk NTS. *Appl. Radiat.*
569 *Isot.* 67, 884–8. <https://doi.org/10.1016/j.apradiso.2009.01.051>
570 Cowper, M., 2009. Analysis of Beach Monitoring Finds – Final Report Issue 1: Report to Sellafield Ltd,
571 Serco.
572 Dale, P., 2013. Dalgety Bay Radioactive Contaminated Land Risk Assessment, Scottish Environment
573 Protection Agency.
574 Dale, P., Robertson, I., Toner, M., 2008. Radioactive particles in dose assessments. *J. Environ.*
575 *Radioact.* 99, 1589–95. <https://doi.org/10.1016/j.jenvrad.2008.06.005>
576 Eriksson, M., Osán, J., Jernström, J., Wegrzynek, D., Simon, R., China-Cano, E., Markowicz, A.,
577 Bamford, S., Tamborini, G., Török, S., Falkenberg, G., Alsecz, A., Dahlgaard, H., Wobruschek,
578 P., Strelci, C., Zoeger, N., Betti, M., 2005. Source term identification of environmental
579 radioactive Pu/U particles by their characterization with non-destructive spectrochemical
580 analytical techniques. *Spectrochim. Acta Part B At. Spectrosc.* 60, 455–469.
581 <https://doi.org/10.1016/j.sab.2005.02.023>
582 IAEA, 2014. Radiation Protection and Safety of Radiation Sources: International Basic Safety
583 Standards.
584 IAEA, 2011. Radioactive particles in the Environment: Sources, Particle Characterization and
585 Analytical Techniques, International Atomic Energy Agency.
586 ICRP, 2007. The 2007 Recommendations of the International Commission on Radiological Protection.
587 ICRP Publication 103., *Annals of the ICRP*.
588 J. Darley, P., W. Charles, M., P. Fell, T., D. Harrison, J., 2003. Doses and risks from the ingestion of
589 Dounreay fuel fragments. *Radiat. Prot. Dosimetry* 105, 49–54.
590 Jernström, J., Eriksson, M., Simon, R., Tamborini, G., Bildstein, O., Marquez, R.C., Kehl, S.R.,
591 Hamilton, T.F., Ranebo, Y., Betti, M., 2006. Characterization and source term assessments of
592 radioactive particles from Marshall Islands using non-destructive analytical techniques.
593 *Spectrochim. Acta Part B At. Spectrosc.* 61, 971–979.
594 <https://doi.org/10.1016/j.sab.2006.09.002>
595 Jimenez-Ramos, M.C., Eriksson, M., García-López, J., Ranebo, Y., García-Tenorio, R., Betti, M., Holm,
596 E., 2010. A comparison of two micro-beam X-ray emission techniques for actinide elemental
597 distribution in microscopic particles originating from the hydrogen bombs involved in the
598 Palomares (Spain) and Thule (Greenland) accidents. *Spectrochim. Acta Part B At. Spectrosc.* 65,
599 823–829. <https://doi.org/10.1016/j.sab.2010.08.001>
600 Jiménez-Ramos, M.C., García-Tenorio, R., Vioque, I., Manjón, G., García-León, M., 2006. Presence of
601 plutonium contamination in soils from Palomares (Spain). *Environ. Pollut.* 142, 487–92.
602 <https://doi.org/10.1016/j.envpol.2005.10.030>
603 Jiménez-Ramos, M.C., García López, J., Eriksson, M., Jernstrom, J., García-Tenorio, R., 2012. PIXE
604 analysis of U and Pu from hot particles: K-lines vs L-lines. *Nucl. Instruments Methods Phys. Res.*
605 *Sect. B Beam Interact. with Mater. Atoms* 273, 118–121.
606 <https://doi.org/10.1016/j.nimb.2011.07.054>
607 Jiménez-Ramos, M.C., Vioque, I., García-Tenorio, R., García León, M., 2008. Levels, distribution and
608 bioavailability of transuranic elements released in the Palomares accident (Spain). *Appl. Radiat.*
609 *Isot.* 66, 1679–82. <https://doi.org/10.1016/j.apradiso.2007.12.015>
610 Kaltofen, M., Gundersen, A., 2017. Radioactively-hot particles detected in dusts and soils from
611 Northern Japan by combination of gamma spectrometry, autoradiography, and SEM/EDS

612 analysis and implications in radiation risk assessment. *Sci. Total Environ.* 607–608, 1065–1072.
613 <https://doi.org/10.1016/J.SCITOTENV.2017.07.091>

614 Lind, O.C., Salbu, B., Janssens, K., Proost, K., Dahlgaard, H., 2005. Characterization of uranium and
615 plutonium containing particles originating from the nuclear weapons accident in Thule,
616 Greenland, 1968. *J. Environ. Radioact.* 81, 21–32.
617 <https://doi.org/10.1016/j.jenvrad.2004.10.013>

618 Lind, O.C., Salbu, B., Janssens, K., Proost, K., García-León, M., García-Tenorio, R., 2007.
619 Characterization of U/Pu particles originating from the nuclear weapon accidents at Palomares,
620 Spain, 1966 and Thule, Greenland, 1968. *Sci. Total Environ.* 376, 294–305.
621 <https://doi.org/10.1016/j.scitotenv.2006.11.050>

622 Lind, O.C., Salbu, B., Skipperud, L., Janssens, K., Jaroszewicz, J., De Nolf, W., 2009. Solid state
623 speciation and potential bioavailability of depleted uranium particles from Kosovo and Kuwait.
624 *J. Environ. Radioact.* 100, 301–7. <https://doi.org/10.1016/j.jenvrad.2008.12.018>

625 López, J.G., Jiménez-Ramos, M.C., García-León, M., García-Tenorio, R., 2007. Characterisation of hot
626 particles remaining in soils from Palomares (Spain) using a nuclear microprobe. *Nucl.*
627 *Instruments Methods Phys. Res. Sect. B Beam Interact. with Mater. Atoms* 260, 343–348.
628 <https://doi.org/10.1016/j.nimb.2007.02.044>

629 Martin, P.G., Griffiths, I., Jones, C.P., Stitt, C.A., Davies-Milner, M., Mosselmans, J.F.W., Yamashiki, Y.,
630 Richards, D.A., Scott, T.B., 2016. In-situ removal and characterisation of uranium-containing
631 particles from sediments surrounding the Fukushima Daiichi Nuclear Power Plant. *Spectrochim.*
632 *Acta Part B At. Spectrosc.* 117, 1–7. <https://doi.org/10.1016/j.sab.2015.12.010>

633 Patton, N., 2013. Dalgety Bay Appropriate Person Report, Scottish Environment Protection Agency.

634 Pöllänen, R., Ketterer, M.E., Lehto, S., Hokkanen, M., Ikäheimonen, T.K., Siiskonen, T., Moring, M.,
635 Rubio Montero, M.P., Martín Sánchez, A., 2006. Multi-technique characterization of a nuclear
636 bomb particle from the Palomares accident. *J. Environ. Radioact.* 90, 15–28.
637 <https://doi.org/10.1016/j.jenvrad.2006.06.007>

638 Pöml, P., Burakov, B., 2017. Study of a “hot” particle with a matrix of U-bearing metallic Zr: Clue to
639 supercriticality during the Chernobyl nuclear accident. *J. Nucl. Mater.* 488, 314–318.
640 <https://doi.org/10.1016/J.JNUCMAT.2017.01.041>

641 Sajih, M., Livens, F.R., Alvarez, R., Morgan, M., 2010. Physicochemical characterisation of depleted
642 uranium (DU) particles at a UK firing test range. *Sci. Total Environ.* 408, 5990–6.
643 <https://doi.org/10.1016/j.scitotenv.2010.07.075>

644 Salbu, B., Janssens, K., Lind, O., Proost, K., Danesi, P., 2003. Oxidation states of uranium in DU
645 particles from Kosovo. *J. Environ. Radioact.* 64, 167–173. [https://doi.org/10.1016/S0265-931X\(02\)00047-4](https://doi.org/10.1016/S0265-931X(02)00047-4)

646

647 Salbu, B., Janssens, K., Lind, O.C., Proost, K., Gijssels, L., Danesi, P.R., 2005. Oxidation states of
648 uranium in depleted uranium particles from Kuwait. *J. Environ. Radioact.* 78, 125–35.
649 <https://doi.org/10.1016/j.jenvrad.2004.04.001>

650 Scottish Government, 2010. The Radioactive Contaminated Land (Scotland) Regulations 2007
651 Statutory Guidance.

652 Shiryayev, A.A., Vlasova, I.E., Yapaskurt, V.O., Burakov, B.E., Averin, A.A., Elantsev, I., 2018. Forensic
653 study of early stages of the Chernobyl accident: Story of three hot particles. *J. Nucl. Mater.* 511,
654 83–90. <https://doi.org/10.1016/J.JNUCMAT.2018.09.003>

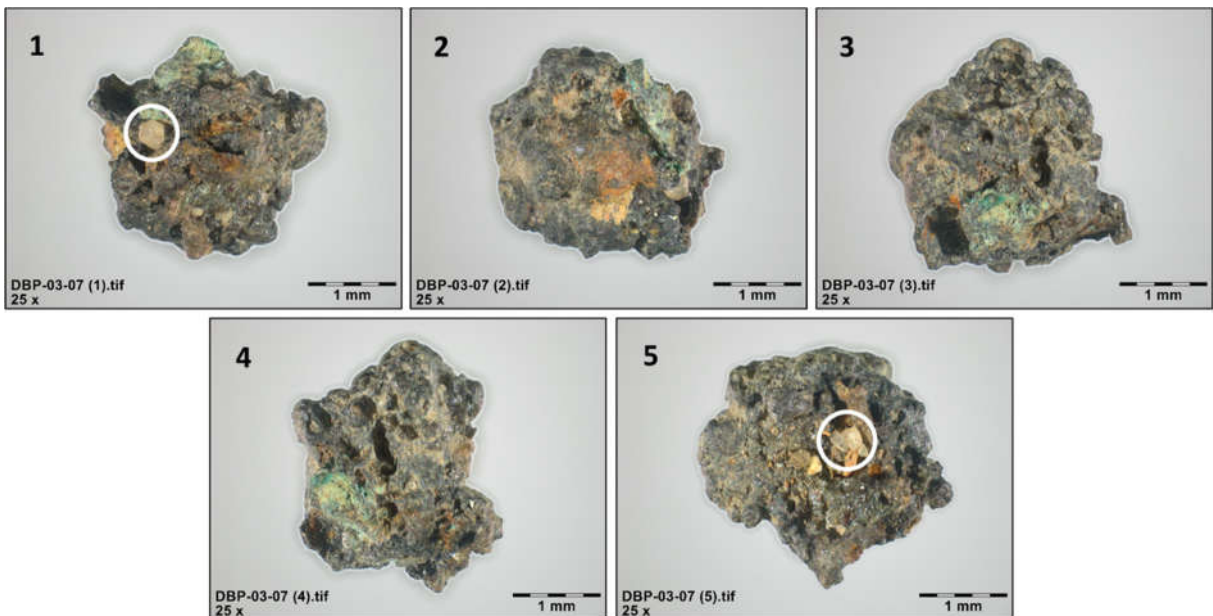
655 Török, S., Osán, J., Vincze, L., Kurunczi, S., Tamborini, G., Betti, M., 2004. Characterization and
656 speciation of depleted uranium in individual soil particles using microanalytical methods.
657 *Spectrochim. Acta Part B At. Spectrosc.* 59, 689–699.
658 <https://doi.org/10.1016/j.sab.2004.02.003>

659 Tyler, A.N., Dale, P., Copplestone, D., Bradley, S., Ewen, H., McGuire, C., Scott, E.M., 2013. The
660 radium legacy: Contaminated land and the committed effective dose from the ingestion of
661 radium contaminated materials. *Environ. Int.* 59, 449–55.
662 <https://doi.org/10.1016/j.envint.2013.06.016>

663 Wilson, C.A., Adderley, W.P., Tyler, A.N., Dale, P., 2013. Characterising the morphological properties
 664 and surface composition of radium contaminated particles: a means of interpreting origin and
 665 deposition. Environ. Sci. Process. Impacts 15, 1921–9. <https://doi.org/10.1039/c3em00141e>
 666 Yamaguchi, N., Mitome, M., Kotone, A.H., Asano, M., Adachi, K., Kogure, T., 2016. Internal structure
 667 of cesium-bearing radioactive microparticles released from Fukushima nuclear power plant. Sci.
 668 Rep. 6, 20548. <https://doi.org/10.1038/srep20548>
 669
 670



671
 672 **Figure 1:** Dalgety Bay showing length of coastline where Ra-226 particles are found (red line = ~850m)
 673
 674



675
 676 **Figure 2:** Optical macroscopy images of Dalgety Bay Ra-226 particle, DBP-03-07, in five different
 677 orientations (White circles = sand grains) (Scale bar = 1mm)
 678
 679
 680
 681

Table 1: Size measurements for Dalgety Bay Ra-226 particle, DBP-03-07

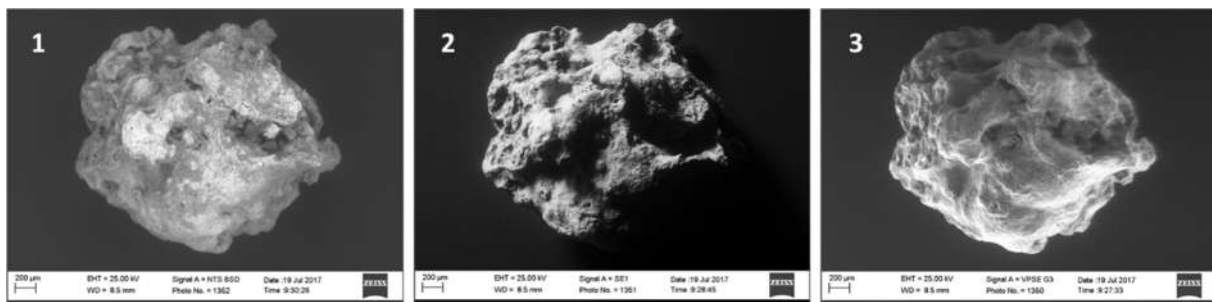
Particle	Radius (mm)	Diameter (mm)	Equivalent Circular Diameter (mm)	Area (mm ²)	Perimeter (mm)
DBP-03-07 (1)	1.189	2.378	2.382	4.457	18.513
DBP-03-07 (2)	1.219	2.438	2.447	4.703	15.41
DBP-03-07 (3)	1.254	2.508	2.519	4.984	17.345
DBP-03-07 (4)	1.199	2.397	2.434	4.653	17.812
DBP-03-07 (5)	1.279	2.558	2.56	5.146	16.755
Mean	1.228	2.456	2.468	4.789	17.167
Standard Deviation	0.038	0.076	0.071	0.275	1.174

682
683

Table 2: Shape measurements for Dalgety Bay Ra-226 particle, DBP-03-07

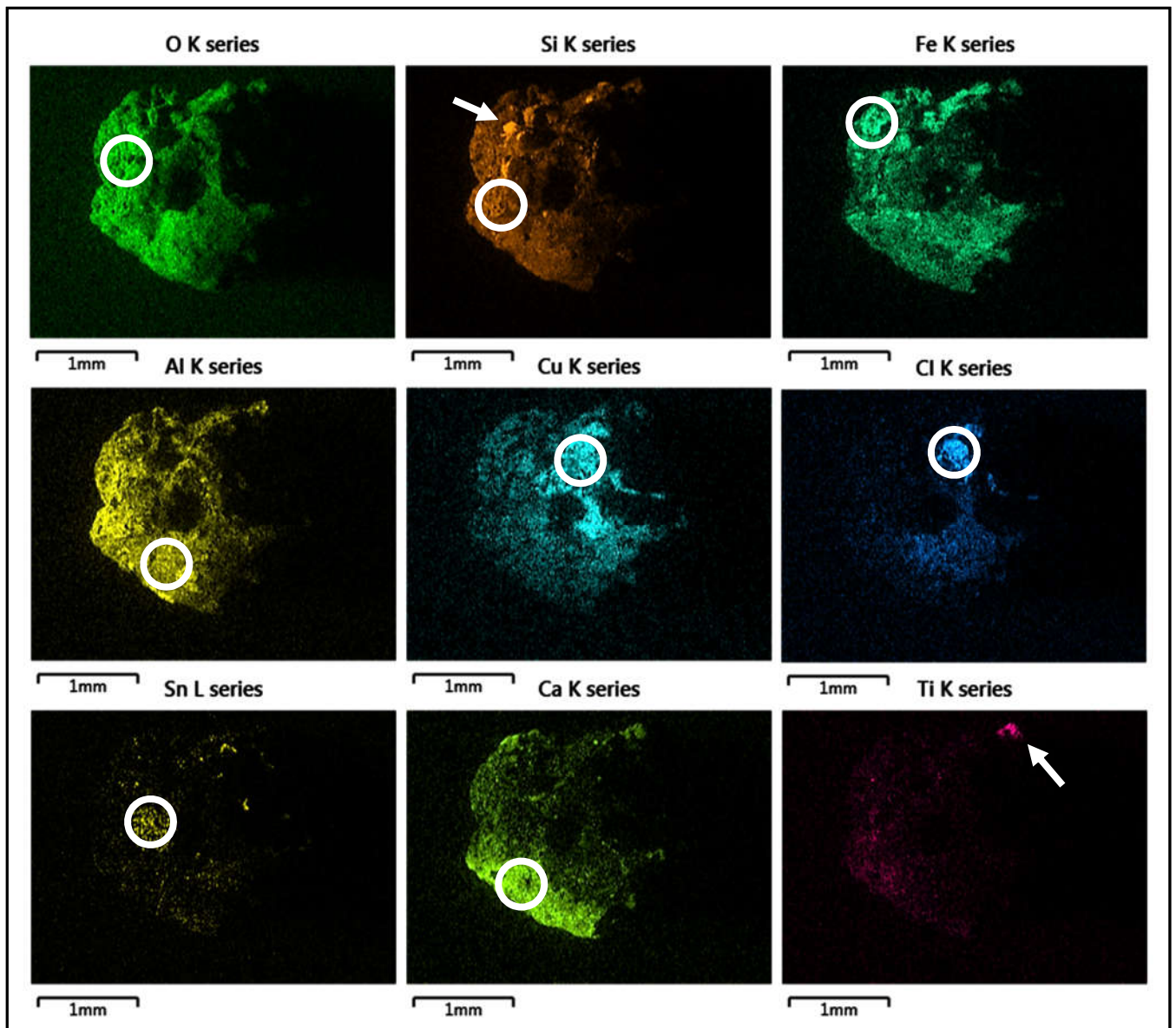
Particle	Shape Factor	Sphericity	Aspect Ratio	Elongation	Convexity
DBP-03-07 (1)	0.163	0.862	1.126	1.077	0.893
DBP-03-07 (2)	0.249	0.741	1.16	1.161	0.927
DBP-03-07 (3)	0.208	0.937	1.1	1.033	0.929
DBP-03-07 (4)	0.184	0.688	1.25	1.206	0.868
DBP-03-07 (5)	0.23	0.771	1.149	1.139	0.92
Mean	0.207	0.8	1.157	1.123	0.908
Standard Deviation	0.034	0.099	0.057	0.069	0.026

684
685
686



687
688
689
690
691
692

Figure 3: (1) Backscattered Electron (BSE), (2) Secondary Electron (SE) and (3) Variable Pressure Secondary Electron (VPSE) images of Dalgety Bay Ra-226 particle, DBP-03-07



693

694

695 **Figure 4:** Energy dispersive X-ray spectroscopy (EDS) element distribution maps of Dalgety Bay Ra-226

696 particle, DBP-03-07 (White circles = phase spectra; Arrows = point spectra)

697

Table 3: Surface chemical composition (weight %) of Dalgety Bay Ra-226 particle, DBP-03-07
 (The highest value for each element is italicised and in bold. If an element is not present in a spectrum it is shown as zero.)

Element	Whole Particle	Al Phase	Cu Phase	Fe Phase	Ca Phase	Sn Phase	Cl Phase	Si Point	Ti Point
O	42.0	49.0	33.7	31.6	51.6	39.6	42.2	57.2	49.6
Fe	12.4	9.1	5.9	26.9	9.8	7.8	3.8	3.0	11.5
Si	12.2	18.4	7.2	7.7	13.9	11.1	7.3	34.8	8.6
Cu	11.1	2.6	41.4	11.3	3.0	4.6	35.2	1.1	3.3
Al	6.9	7.5	0.0	6.1	6.9	6.1	0.0	1.9	5.3
Ca	3.1	4.0	1.1	3.6	9.2	1.7	0.6	0.4	4.7
Mg	2.6	1.8	6.8	3.9	1.8	1.3	0.0	0.5	1.4
Sn	2.0	0.0	0.0	0.0	0.0	11.9	0.0	0.0	1.0
Cl	1.3	0.4	2.2	2.2	0.3	0.2	9.9	0.1	0.0
Na	1.2	2.5	0.0	1.4	0.0	1.9	0.0	0.6	0.8
Zn	0.8	0.3	0.8	2.0	0.9	1.0	0.0	0.0	0.3
Pb	0.8	0.0	0.0	1.4	0.8	0.9	0.0	0.0	0.0
K	0.7	1.1	0.3	0.0	0.0	1.0	0.5	0.2	0.4
Ti	0.6	1.0	0.2	0.0	0.7	1.0	0.1	0.2	10.7
Ta	0.6	0.0	0.0	0.0	0.0	0.0	0.0	0.0	0.0
P	0.5	0.5	0.0	0.4	0.7	0.4	0.0	0.0	2.0
Ni	0.5	0.2	0.5	0.5	0.2	0.2	0.4	0.0	0.1
Mn	0.5	0.7	0.0	0.3	0.0	0.6	0.0	0.0	0.3
S	0.4	0.2	0.0	0.5	0.3	0.0	0.0	0.0	0.0
Sb	0.0	0.0	0.0	0.0	0.0	8.8	0.0	0.0	0.0
Ba	0.0	0.9	0.0	0.0	0.0	0.0	0.0	0.0	0.0
Total	100	100	100	100	100	100	100	100	100